

# SYNTHESIS OF METASTABLE ALLOYS BY ION MIXING IN THE BINARY METAL SYSTEMS AND THEORETICAL MODELLING

B.X.Liu, Z.J.Zhang, O.Jin and F.Pan

Department of Materials Science and Engineering, Tsinghua University, Beijing 100084, Center of Condensed Matter and Radiation Physics, CCAST (World Lab.), Beijing 100080, CHINA.

## ABSTRACT

(1) The metastable crystalline (MX) phases formed by ion mixing are classified into 5 types, i.e. the super-saturated solid solutions and the enlarged HCP-I phases reported earlier, and the newly observed FCC-I phases in hcp-based alloys, The FCC-II and HCP-II phases in bcc-based alloys. The growth kinetics of the MX phases is discussed. (2) The interfacial free energy in the multilayered films was found to play an important role in ion beam mixing (IM) induced amorphization. By adding sufficient interfaces, amorphous alloys were obtained even in the systems with rather positive heat of formation. (3) Gibbs free energy diagrams of some representative systems were constructed, by calculating the free energy curves of all the competing phases. Steady-state thermal annealing was conducted and the results confirmed the relevance of the constructed diagrams, which were in turn employed to interpret the MX phase formation as well as the glass forming ability upon IM in the binary metal systems.

## 1. INTRODUCTION

Ion beam mixing of multilayered films was introduced in early 1980s [1] and has been employed to study the formation of various metastable phases [2,3,4]. Up to date, some 75 binary metal systems have been investigated and a great number of new amorphous and metastable crystalline alloys has been obtained by IM [5]. Based on the experimental data, several empirical models [6,7,8] have been proposed to predict the glass forming ability (GFA). Concerning the MX phase formation, more experimental studies are needed to gain a comprehensive view. In the theoretical pursuing, the free energy diagrams of some alloy systems with negative heat of formation ( $\Delta H_F$ ) were constructed based on Miedema's model [9] and the methods developed by J.A.Alonso [10]. In this respect, there are two open questions, i.e. correct calculation of the free energy curves for the MX phases, and the role of interfacial free energy in IM induced amorphization for the systems with positive  $\Delta H_F$ . Besides, the growth kinetics of the MX phase should be further clarified. These issues have been studied very recently by authors' group and this paper is to present a brief summary of IM synthesis of the metastable alloys together with our recent results.

## 2. EXPERIMENTAL PROCEDURE

Multilayered films were prepared by alternatively depositing pure metals A and B onto NaCl single crystals as substrates in an electron-gun evaporation system with a vacuum level on the order of  $10^{-7}$  Torr. The total thickness of the films was 40-70 nm, which was designed to equal projected range plus projected range straggling of the irradiation ions, typically 200 or 300 keV xenon ions. The relative thicknesses were adjusted to obtain the desired compositions and each sample frequently consisted of 5-9 metal layers. The as-deposited films were then irradiated at room temperature to the doses ranging from  $3 \times 10^{14}$  to  $1 \times 10^{16}$  Xe/cm<sup>2</sup>. The vacuum of the implanter was on the order of  $10^{-6}$  Torr. To minimize beam heating, the ion current density was controlled to be 1-2  $\mu$ A/cm<sup>2</sup>, and the average temperature of the films was estimated to be within 100-150 °C. Transmission electron microscopy (TEM) and selected area diffraction (SAD) were employed to identify the structure of the resultant phases, of which the compositions were determined by energy dispersive spectrum (EDS) with an experimental error of 5%.

## 3. METASTABLE CRYSTALLINE PHASE FORMATION AND GROWTH KINETICS

In addition to two types of MX phases reported earlier, i.e. the super-saturated solid solutions [3] and the enlarged HCP-I phases having a composition at  $A_3B$  observed in Ti-Au, Co-Au, Co-Mo, (hcp-based), Ni-Mo and Ni-Nb (fcc-based) systems [4], three types of new MX phases were formed by IM. Table I lists the formation of the FCC-I phases by IM in some hcp-based binary metal systems with a composition very close to the hcp metals. Table II shows the formation of another FCC-II phases by IM in some bcc-based alloys with a stoichiometry of  $AB_{3-4}$ . Further IM studies revealed that the FCC-II phase was formed through a two-step transition from hcp to fcc via an intermediate state of hcp structure, which can be considered as another new MX phase named as HCP-II also at  $AB_{3-4}$  [11].

Table I. Fcc-I MX phases formed in binary transition metal systems induced by room temperature 200 keV xenon ion mixing. (Note: dose in  $10^{14}$  Xe<sup>+</sup>/cm<sup>2</sup>).

System and Composition	mixing dose	lattice parameter (Å)
Co <sub>94</sub> Mo <sub>6</sub> ~Co <sub>87</sub> Mo <sub>13</sub>	30	3.55~3.60
Co <sub>98</sub> Ta <sub>2</sub> ~Co <sub>80</sub> Ta <sub>20</sub>	30	3.55~3.65
Y <sub>73</sub> Mo <sub>27</sub> ~Y <sub>83</sub> Mo <sub>17</sub>	70	5.10
Y <sub>85</sub> Ta <sub>15</sub> ~Y <sub>75</sub> Ta <sub>25</sub>	10	5.18
Y <sub>99</sub> Zr <sub>1</sub> ~Y <sub>70</sub> Zr <sub>30</sub>	50	4.96
Y <sub>75</sub> Zr <sub>25</sub> ~Y <sub>85</sub> Zr <sub>15</sub>	30	4.67
Zr <sub>68</sub> Nb <sub>32</sub> ~Zr <sub>88</sub> Nb <sub>12</sub>	7	4.35~4.80

Table II. Fcc-II MX phases formed in the bcc-based binary metals around  $AB_{3-4}$ , where B is the bcc metal, through a two-step transition of  $bcc \rightarrow hcp \rightarrow fcc$  induced by room temperature 200 keV xenon ion beam mixing. (Note: hcp-II is the intermediate state in the transition and is another MX phase).

A-B (B=bcc)	System and composition	hcp-II obtained	Forming Dose	fcc-II obtained	Forming Dose
fcc-bcc	Ni <sub>23</sub> Mo <sub>77</sub>	Yes	$9 \times 10^{14}$	Yes	$7 \times 10^{15}$
	Ni <sub>20</sub> Nb <sub>80</sub>	Yes	$1 \times 10^{15}$	Yes	$7 \times 10^{15}$
	Ni <sub>25</sub> Ta <sub>75</sub>	No	-----	Yes	$7 \times 10^{14}$
hcp-bcc	Co <sub>20</sub> Mo <sub>80</sub>	Yes	$7 \times 10^{14}$	Yes	$5 \times 10^{15}$
	Co <sub>23</sub> Nb <sub>77</sub>	Yes	$9 \times 10^{14}$	Yes	$7 \times 10^{15}$
	Co <sub>25</sub> Ta <sub>75</sub>	No	-----	Yes	$5 \times 10^{15}$
	Y <sub>22</sub> Mo <sub>78</sub>	Yes	$3 \times 10^{15}$	Yes	$5 \times 10^{15}$
	Y <sub>25</sub> Ta <sub>75</sub>	Yes	$3 \times 10^{15}$	Yes	$7 \times 10^{15}$
	Zr <sub>7</sub> Mo <sub>93</sub>	Yes	$1 \times 10^{15}$	Yes	$5 \times 10^{15}$
	Zr <sub>19</sub> Nb <sub>81</sub>	No	-----	Yes	$7 \times 10^{14}$
	Zr <sub>20</sub> Ta <sub>80</sub>	No	-----	Yes	$7 \times 10^{15}$
bcc-bcc	Fe <sub>24</sub> Mo <sub>76</sub>	Yes	$9 \times 10^{14}$	Yes	$7 \times 10^{15}$
	Fe <sub>20</sub> Nb <sub>80</sub>	Yes	$9 \times 10^{14}$	Yes	$7 \times 10^{15}$
	Fe <sub>20</sub> Ta <sub>80</sub>	No	-----	Yes	$5 \times 10^{15}$

It is commonly accepted that the growth of the MX phase in IM process is completed in the relaxation period after the atomic collision cascade triggered by ion irradiation and that relaxation only lasts for  $10^{-10}$ - $10^{-9}$  sec [12], which allows only simple crystalline structure to grow and it is indeed the case for all the formed MX phases by IM. The growth of the MX phases was therefore simply through three fast transition units or their combinations, i.e. hcp-fcc, fcc-hcp and bcc-hcp. For the hcp-fcc transition, a sliding of atoms on the planes parallel to the  $(0002)_{hcp}$  plane along  $\langle 1100 \rangle_{hcp}$  directions by a vector of  $1/3[1100]_{hcp}$  transforms easily the hcp structure into fcc, and its reverse procedure is the one for fcc-hcp. While for the bcc-hcp transition, in a shearing mechanism, the  $(111)_{bcc}$  acted as the habit plane, and  $[111]_{bcc}$  (or  $[2110]_{hcp}$ ) acted as the shearing axis. The formation of the FCC-II phases was through a two-step transition, i.e. first bcc-hcp and then hcp-fcc. Accordingly, the lattice parameters of the FCC-II and HCP-II phases were deduced and were in good agreement with the experimental results [11,13].

#### 4. ROLE OF INTERFACE IN AMORPHOUS ALLOY FORMATION

It has been estimated that an effective cooling speed can be as high as  $10^{13}$ - $10^{14}$  K/sec. in IM process [12], which is much greater than that in liquid melt quenching. As a result, IM can greatly extend the GFA of the binary metal systems. In fact, in

the systems with negative  $\Delta H_F$ , IM is possible to produce amorphous alloys in a broad composition range except the solid solution regions [14]. One intrinsic parameter was proposed by B.X.Liu [15] for a measure of GFA, i.e. the MPAR (abbreviation for maximum possible amorphization range), which is the total width of the two-phase regions observed from the equilibrium phase diagram and equals 100% (as the whole composition range) minus the maximum solubility at two metal sides. The second parameter was the heat of formation  $\Delta H_F$  suggested firstly by Alonso [16], and its effect, however, has been debated for some times. Although the authors' group has demonstrated by IM experiments that a positive  $\Delta H_F$  did not strictly prevent glass from forming like Alonso predicted, but only limited amorphization in a narrow composition range [15,4], a reasonable thermodynamic interpretation has been lacking and is still an open question.

To give a relevant answer, comparison of the free energy curve of the amorphous phase with the initial energetic state of the multilayered films is necessary. The Y-Mo system selected to discuss this issue is essentially an immiscible one with a rather positive  $\Delta H_F$  of +35 kJ/mol. Figure 1 is the calculated free energy diagram based on the methods described in well documented literature [9,10]. One can see that the shape of the free energy curve of the amorphous phase is convex, which is sharply different from the concave shape always seen for the systems with negative  $\Delta H_F$ . Obviously, amorphous phase has higher than that of a mixture of Y and Mo crystalline phases, and is energetically unfavored to be formed. Note that the energy of the mixture is not the energetic state of the multilayered films, in which the excess free energy originating from the interfaces was not included yet.

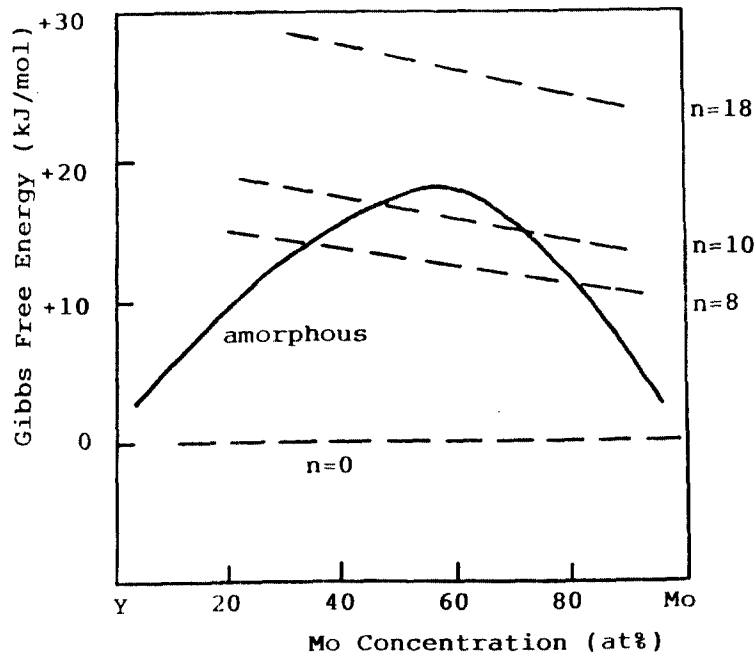


Figure 1. A calculated free energy diagram of the Y-Mo system with  $\Delta H_F$  exceeding +35 kJ/mol. The dashed lines represent the initial energetic states of the as-deposited Y-Mo multilayered films including 8, 10 and 18 interfaces, respectively.

Naturally, the atoms in the interfaces are in a metastable configuration and can possess higher energy than those in the bulk form. According to Miedema, the excess enthalpy of one mole interfacial atoms is  $\Delta H = S^F \times \gamma^F$ , where  $S^F$  is the surface area occupied by the interfacial atoms,  $\gamma^F$  is the ratio energy of the interface [17]. Assuming the entropy term plays a minor role, and an interface thickness is 5 Å, the excess free energy as a function of the number (N) of interfaces, or more precisely the fraction of interfacial atoms, was calculated and added to energetic state of the multilayered films. For the cases of N=8, 10 and 18, the initial free energy curves of the Y-Mo multilayers were calculated and are added in Figure 1 by dashed lines. It is obvious that with increasing the number of interface, the free energy curves (N=8 and 10) of the multilayered films (N=8 and 10) are raised to intersect with that of the amorphous phase, dividing the composition range into three parts, two regimes favouring amorphization close to two metal sides and another unfavouring one in central portion, and that it eventually becomes higher than that of the amorphous state over the whole composition range when N=18.

Table III lists the predictions for IM induced amorphization and the experimental results in the Y-Mo system. When N=8, amorphization was achieved at two separated compositions of  $Y_{80}Mo_{20}$  and  $Y_{20}Mo_{80}$ , and this similar behaviour has been observed in some other systems, e.g. in Fe-Cu (+19 kJ/mol)[18,19] and Zr-Nb (+7 kJ/mol)[20] systems. When N=18, amorphous alloys were also obtained at mid-composition, i.e. at  $Y_{50}Mo_{50}$ ,  $Y_{40}Mo_{60}$  and  $Y_{60}Mo_{40}$ . These results were in excellent agreement with the prediction based on interface consideration. More interestingly, as the  $Y_{50}Mo_{50}$  multilayered films containing 18 interfaces have higher energy than that of the amorphous state, the films should undergo amorphous upon heating, which was confirmed by thermal annealing of the films at 350 °C for 2 hours. To our knowledge, this is the first observation of spontaneous vitrification generated by interface in the systems of rather positive  $\Delta H_F$  [21], which has been considered to be impossible according to Schwarz and Johnson [22].

Table III. Predicted composition ranges favouring amorphization of the Y-Mo multilayered films with various numbers of interfaces based on the calculations and the confirmation by the experimental results. In the table,  $\alpha$  is the fraction of interfacial atoms versus the total atoms in the multilayered films. (Note: For n=18 multilayers, two compositions denoted by "\*" were not checked, as it was not necessary.)

Interfaces	Composition	$Y_{80}Mo_{20}$	$Y_{60}Mo_{40}$	$Y_{50}Mo_{50}$	$Y_{40}Mo_{60}$	$Y_{20}Mo_{80}$
n=18 $\alpha=18.1$ at%	predicted	Yes	Yes	Yes	Yes	Yes
	obtained	*	Yes	Yes	Yes	*
n=10 $\alpha=10$ at%	predicted	Yes	Yes	No	No	Yes
	obtained	Yes	Yes	No	No	Yes
n=8 $\alpha=8.1$ at%	predicted	Yes	No	No	No	Yes
	obtained	Yes	No	No	No	Yes

## 5. THERMODYNAMICS OF THE METASTABLE ALLOY FORMATION

The emphasis of this section is to calculate the free energy curves of the newly formed MX phases, among which the HCP-I, HCP-II and FCC-II phases are discussed in detail. The enthalpy change of the MX phase is expressed by  $\Delta H = \Delta H_c + \Delta H_e + \Delta H_s$ , where  $\Delta H_c$ ,  $\Delta H_e$  and  $\Delta H_s$  are chemical, elastic and structural contributions to the change of enthalpy, respectively. As the HCP-I phase was formed at a composition of  $A_3B$  near an equilibrium compound, and the structure of the HCP-I was different from the corresponding compound, the elastic energy raised from the structural difference should be calculated and included. While for the FCC-II and HCP-II phases formed at the composition around  $AB_{3/4}$ , where existed no equilibrium compound of different structure, the elastic energy can be relaxed to a minimum due to the ordered arrangement of the atoms ( $\Delta H_e$  is negligible). Accordingly, a typical free energy diagram was constructed for the Ni-Nb system as a representative one and is shown in Figure 2.

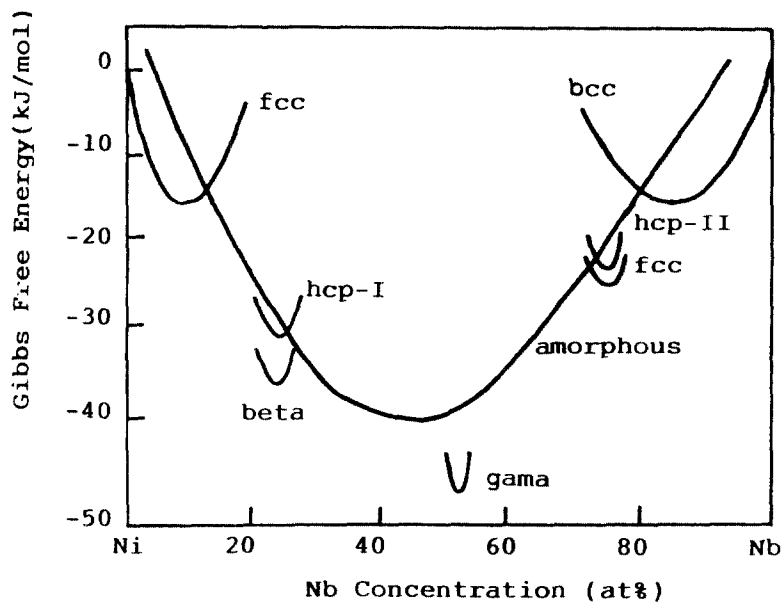


Figure 2. A calculated free energy diagram of the Ni-Nb system, in which the free energy curves of the hcp-I, hcp-II and fcc-II MX phases are included.

Before applying the constructed diagram to discuss IM induced alloying, a fundamental and long debated question should be answered, i.e. the relevance of the calculated results based on Miedema's theory, which is still at a semi-quantitative stage. The authors suggested recently, for the first time, an experimental method to confirm the relevance of the calculation, i.e. steady-state thermal annealing of multilayered films at selected compositions. As the multilayered films are in a higher free energy state, they should relax down to the states of lower free energy during annealing and the sequence of phase evolution with increasing temperature can give a relative measure of the energetic states of the competing phases. Generally, the phase

appearing at lower temperature has higher energy than that of the phase appearing at higher temperature. Take  $\text{Ni}_{20}\text{Nb}_{80}$  multilayered films as example, the phase appearance sequence upon annealing with increasing temperature is solid solution, HCP-II, FCC-II and eventually the corresponding equilibrium state, which is exact the same as that deduced from the calculated free energy curves of the phases. Similar results were also obtained at other compositions of interest as well as in other systems. We thus believe that the constructed free energy diagrams are correct at least in their outline, though the precision of the calculation needs further studies.

From the calculated diagram of the Ni-Nb system, one sees that the free energy of the amorphous phase is lower than that of the solid solution within a composition range from 20 to 80 at% of Nb, which agrees well with the ion mixing results that amorphous alloys have been obtained within a composition range from 25 to 80 at% of Nb. Interestingly, the free energy curves of the HCP-I phase and the amorphous phase intersect each other along the composition axis, indicating at certain composition the transformation of MX HCP-I phase into amorphous upon heating is possible. Such phase transition was indeed observed in the Ni-Nb system [23] and some other systems [24] by authors' group, and can also be considered as spontaneous vitrification beginning with MX phase.

## VI. CONCLUDING REMARKS

1. IM has so far formed five types of MX phases based on three major structures of hcp, fcc and bcc. It is therefore possible to predict the MX phase formation by the established structural correlation.

2. Amorphous alloys can be obtained by IM even in the binary metal systems with rather positive  $H_F$  in a flexible composition range, by properly designing the fraction of interfacial atoms in the multilayered films.

3. The free energy diagram calculated by Miedema's model and Alonso's method was proved by steady-state thermal annealing of multilayers to be relevant in its outline and can give reasonable interpretation to the formation of metastable alloys by IM.

## REFERENCES

1. B.Y.Tsaur, PhD Thesis, California Institute of Technology, 1980.
2. B.X.Liu, W.L.Johnson, M-A.Nicolet and S.S.Lau, Appl.Phys.Lett. 42, (1983) 45.
3. J.W.Mayer, B.Y.Tsaur, S.S.Lau and L.S.Hung, Nucl. Instr. Meth.182/183, (1981) 1.
4. B.X.Liu, Phys. Stat. Sol.(a) 94, (1986) 11.
5. B.X.Liu and Z.J.Zhang, Materials Science and Engineering A179/180, (1994) 189.
6. B.X.Liu, Materials Letters 5, (1987) 322.

7. J.A.Alonso, *Phys. Rev.* B36, (1987) 3716.
8. P.M.Ossi, *Phys. Stat. Sol. (a)* 119, (1990) 463.
9. A.K.Niessen, A.R.Miedema, F.R.De.Boer and R.Boom, *Physica* B151, (1988) 401.
10. J.A.Alonso, L.J.Gallego and J.A.Somozar, *IL Nuovo Cimento* 12, (1990) 587.
11. Z.J.Zhang and B.X.Liu, *J.Appl. Phys.* 75, (1994) 4948.
12. M.W.Thompson, *Defects and Radiation Damage in Metals*, Cambridge University Press, Cambridge, 1969, Chap.4-5.
13. see for example, Z.J.Zhang, O.Jin and B.X.Liu, *Phys. Rev.* B51, (1995) 8076.
14. see for example, B.X.Liu and Z.J.Zhang, *Phys. Rev.* B49, (1994) 12519.
15. B.X.Liu, *Nucl. Instr. Meth. in Phys. Res.* B19/20, (1987) 682.
16. J.A.Alonso and S.Simozar, *Solid State Commun.* 46, (1983) 269.
17. J.Gerkema and A.R.Miedema, *Surface Sci.* 124, (1981) 351.
18. L.J.Huang, B.X.Liu and H-D.Li, *Appl. Phys.* A44, (1987) 269.
19. F.Pan, PhD Theis, Tsinghua University, 1993.
20. O.Jin and B.X.Liu, *J.Phys.:Condensed Matter* 6, (1994) L39.
21. B.X.Liu and Z.J.Zhang, *Phys. Rev. B*, (to be published)
22. R.B.Schwarz and W.L.Johnson, *Phys. Rev. Lett.* 51, (1983) 415.
23. B.X.Liu, H.Y.Bai, Z.J.Zhang and Q.L.Qiu, *J. Alloys and Compounds* 196, (1993) 37.
24. B.X.Liu, Z.J.Zhang and H.Y.Bai, *J.Non-Crystalline Solids* 156-158, (1993) 603.